Journal of Bionic Engineering (2023) 20:858–872
https://doi.org/10.1007/s42235-022-00313-x

REVIEW ARTICLE

Bionic Stepping Motors Driven by Piezoelectric Materials

Shupeng Wang[1] · Shihui Zhou[1] · Xiaolong Zhang[1] · Pengyun Xu[2] · Zhihui Zhang[1] · Luquan Ren[1]

Received: 7 October 2022 / Revised: 20 November 2022 / Accepted: 22 November 2022 / Published online: 6 December 2022

Abstract
By imitating the behavioral characteristics of some typical animals, researchers develop bionic stepping motors to extend the working range of piezoelectric materials and utilize their high accuracy advantage as well. A comprehensive review of the bionic stepping motors driven by piezoelectric materials is presented in this work. The main parts of stepping piezoelectric motors, including the feeding module, clamping module, and other critical components, are introduced elaborately. We classify the bionic stepping piezoelectric motors into inchworm motors, seal motors, and inertia motors depending on their main structure modules, and present the mutual transformation relationships among the three types. In terms of the relative position relationships among the main structure modules, each of the inchworm motors, seal motors, and inertia motors can further be divided into walker type, pusher type, and hybrid type. The configurations and working principles of all bionic stepping piezoelectric motors are reported, followed by a discussion of the advantages and disadvantages of the performance for each type. This work provides theoretical support and thoughtful insights for the understanding, analysis, design, and application of the bionic stepping piezoelectric motors.

Keywords Bionic stepping piezoelectric motor · Inchworm motor · Seal motor · Inertia motor · Walker type · Pusher type · Hybrid type

1 Introduction

As the core unit of energy conversion, motors with excellent performance usually play a crucial role in many scientific and engineering fields [1–3]. Generally, positioning accuracy, working stroke, loading capability, operating velocity, motion resolution, and overall dimensions are the most important performance criteria for high-end motors [4, 5]. Traditional motors, such as internal-combustion engines, electromagnetic motors, hydraulic motors, and pneumatic motors, exhibit many favorable characteristics, including large torque, long working stroke, and high stiffness. However, they can hardly overcome the defects such as oversize volume, accumulation error, motion loss, and wind up [6, 7]. With the rapid rise of technical requirements, traditional motors have been unable to satisfy the modern scientific and engineering fields [6, 7]. The development of next-generation motors with more excellent characteristics has become one of the most active research hotspots [8–12].

Piezoelectric motors driven by piezoelectric materials are developed as time advances. Piezoelectric materials are a kind of smart functional materials which work with the piezoelectric effects including direct piezoelectric effect and inverse piezoelectric effect [13, 14]. The direct piezoelectric effect refers to when deformation occurs under the action of external force, the piezoelectric materials can produce electric charges at the two electrodes [15–17]. On the contrary, the inverse piezoelectric effect is that when we supply electricity to the two electrodes, the piezoelectric materials can generate deformations [15–17]. In general, the direct piezoelectric effect enables the piezoelectric materials to be excellent sensing elements, and the inverse piezoelectric effect can be used to develop precision motors. As actuation materials, the piezoelectric materials mainly exhibit the following advantages: (1) ultra-high accuracy, up to sub-nanometer scale; (2) super-fast response, up to microsecond level; (3) large output force and high mechanical stiffness; (4) no magnetic field interference, no magnetic field generation, and unaffected by the external magnetic field; (5) strong

✉ Zhihui Zhang
zhzh@jlu.edu.cn

[1] Key Laboratory of Bionic Engineering (Ministry of Education), Jilin University, Changchun 130022, China

[2] Department of Mechanical and Electrical Engineering, Ocean University of China, Qingdao 266100, China

adaptability, applicable for the vacuum, and low-temperature environments; (6) no intermediate transmission, no moving pair clearance, and no lubrication required; (7) high electromechanical conversion rate and high energy density; (8) diverse structures, flexible design and easy miniaturization [15–17]. Therefore, both in terms of structures and functions, the piezoelectric materials are excellent actuation components for a new generation of motors.

In recent decades, numerous types of piezoelectric motors have been developed, which have been widely used in the precision drive systems, such as the manipulation of biological specimens, optical element alignment, semiconductor equipment, insect-scaled robots, and micro-positioning stages [15–19]. Meanwhile, strenuous efforts have been made to address the shortcomings of a small strain of piezoelectric materials [18, 19]. First, the piezo-stack with a multilayer structure combined the small strains from many single-layer units into a long output displacement [20, 21]. The work range of piezo-stack motors could reach tens of micrometers [22, 23]. Second, various amplification mechanisms were designed to enlarge the displacement of piezoelectric materials, such as the lever mechanism [24, 25], bridge mechanism [26, 27], Scott-Russell mechanism [28, 29], and bimorph mechanism [30, 31]. By virtue of various amplification mechanisms, the work range of piezoelectric motors could reach hundreds of micrometers [32, 33]. However, this was still insufficient in many applications. Therefore, researchers created different bionic stepping piezoelectric motors by imitating the walking manner of some typical animals [34–36]. According to the practical requirements, the bionic stepping piezoelectric motors were able to accumulate the small displacements of piezoelectric materials and generate a sufficient traveling stroke step by step. With the stepping motion principles, the piezoelectric motors are completely liberated from the small displacement and preserve the main advantages of piezoelectric materials, concurrently. The work range of the bionic stepping piezoelectric motors can reach a millimeter scale or even without limit [34–36].

This work proposes a comprehensive review of bionic stepping piezoelectric motors with cross-scale output performance. The review is outlined in form of rotary piezoelectric motors, while the overall contents cover both the linear motors and rotary motors. Correspondingly, the contents of the review are organized as follows: in Sect. 2, the bionic stepping piezoelectric motors are classified into inchworm motors, seal motors, and inertia motors. In Sect. 3, the classifications, configurations, and working principles of the inchworm piezoelectric motors are introduced. In Sect. 4, we elaborate the classifications, configurations, and working principles of the seal piezoelectric motors. In Sect. 5, the classifications, configurations, and working principles of the inertia piezoelectric motors are presented. The characteristics of the three types of bionic stepping piezoelectric motors are analyzed in Sect. 6. Conclusions of the work are reported in Sect. 7.

2 Overview of the Bionic Stepping Piezoelectric Motors

Bionic stepping piezoelectric motors, just as its name implies, imitate some animals' typical behavioral manners to accumulate the small displacements of piezoelectric materials to generate sufficient working stroke step by step. Generally, a bionic stepping piezoelectric motor contains a feeding module, clamping module, and other key components [34–36]. The feeding module is utilized to produce driving displacements of the rotor while the clamping module is employed to clamp/unclamp the rotor to/from the stator at the appropriate time [34–36]. With the sequential coordination of the feeding module and clamping module, the bionic stepping piezoelectric motor can drive the rotor to output large angular displacements step by step.

It is universally acknowledged that the motors can be called bionic stepping piezoelectric motors provided the feeding module is driven by piezoelectric materials [34–36]. The outputs of the piezoelectric materials are linear displacements including the longitudinal strains, transversal strains, and shear strains, which can all be used to drive the motor. In order to achieve angular displacements of piezoelectric motors, considerable efforts have been made by different researchers. For example, flexure hinges, revolute pairs, and other methods are utilized to transform linear displacements into angular displacements [37–42]. Flexure hinges are a kind of deformable mechanism to guide movements, which consist of flexible parts and rigid parts. The flexible parts with small stiffness and the rigid parts with large stiffness are designed and machined from a single piece of material [37–42]. With the given deformations and constraints of flexible parts, the rigid parts can move at certain degrees of freedom. Owing to the advantages of compliant and repeatable motions, compact structures, small inertial mass, no backlash, and friction, the flexure hinges are widely utilized in piezoelectric motors, especially in stepping piezoelectric motors [37–42]. Furthermore, with the designed flexure hinges mechanisms, we can not only obtain the angular displacements but also multiply and enlarge the small deformations of piezoelectric materials [40–42].

Many clamping methods are reported by the researchers, such as the deformation clamp [43, 44], electromagnet clamp [45, 46], inertia clamp [47, 48], and wedge clamp [49, 50]. The deformation clamp utilizes the deformation of the clamping component to tension rotor into the bearing of stator. With the adhesion force of an electromagnet, the electromagnet clamp can clamp the rotor onto the stator.

The inertia clamp presses the rotor onto the stator with the inertial force generated by a mass block during acceleration. The wedge clamp can clamp the rotor onto the stator with the self-lock effect between a wedge block pair. Since almost all the stepping piezoelectric motors use frictional force to maintain the output thrust, the clamping force determines the capacity of the stepping piezoelectric motors [43–46]. Moreover, because of the contact and separation during the clamping process, the clamping module also influences the stepping piezoelectric motors from the vibration, noise, accuracy, and so on [47–50].

In terms of the main structure modules, as shown in Fig. 1, the bionic stepping piezoelectric motors are classified into inchworm motors [51–53], seal motors [54–56], and inertia motors [57–60]. Each type of these stepping motors can be further divided into walker type, pusher type, and hybrid type. All the bionic stepping piezoelectric motors have specific configurations, working principles, and characteristics. A suitable type of piezoelectric motor can be selected according to the actual demand.

3 Inchworm Piezoelectric Motors

3.1 Inchworm Motion Principle

The inchworm is an arthropod with a slender body and many pairs of feet. The body is flexible and bendable. The feet are on both ends of the body, which are named as fore feet and hind feet respectively. As shown in Fig. 2, the crawling

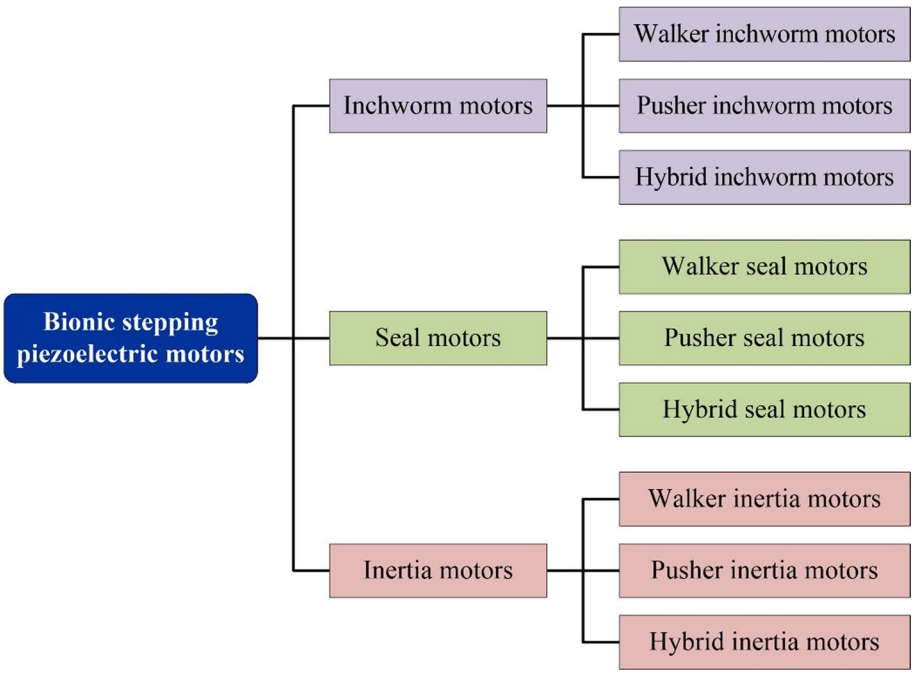

Fig. 1 Classifications of bionic stepping piezoelectric motors

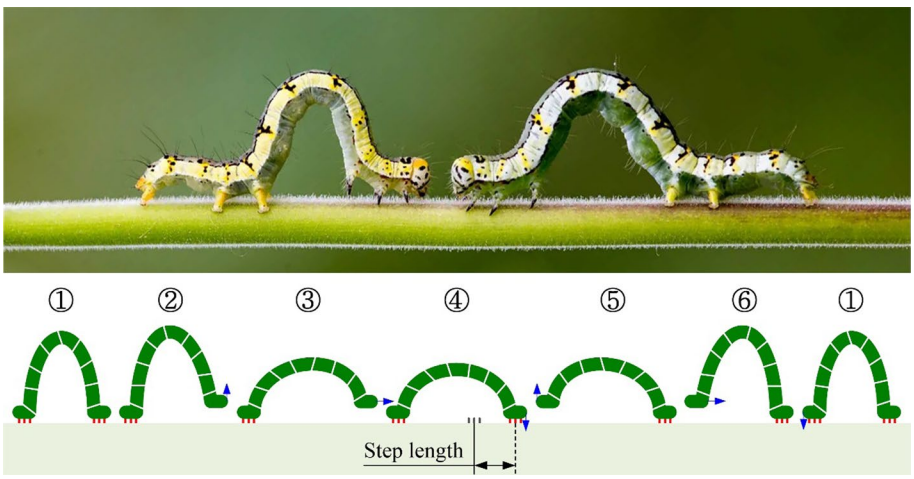

Fig. 2 Stepping motion of the inchworm

manner of the inchworm is a typical stepping motion. The process can be divided into different steps: first, the inchworm grips on the branch with the fore feet and hind feet; second, it releases the fore feet from the branch; third, it straightens the body and pushes forward the fore feet; fourth, it grips on the branch again with the fore feet; fifth, it releases the hind feet from the branch; sixth, it bends the body again and pulls forward the hind feet; lastly, it grips on the branch again with the hind feet. After the above process, the inchworm moves forward one step on the branch and returns back to the initial status (the first step). Obviously, if the above process is repeated time after time, the inchworm can crawl with a long distance on the branch.

Imitating the crawling manner of the inchworm, researchers created the inchworm-type bionic stepping piezoelectric motors. As Fig. 3 shows, the inchworm piezoelectric motors are mainly composed of a feeding module to imitate the bendable body and two clamping modules to imitate the fore feet and the hind feet [51–53]. The feeding module is used to generate the driving angular displacements and the clamping modules are employed to clamp or unclamp the rotor at the right time interval. According to the relative position relationships among the feeding module and the clamping modules, the inchworm piezoelectric motors can be classified into three types, which are named walker inchworm motors (see Fig. 3a), pusher inchworm motors (see Fig. 3b), and hybrid inchworm motors (see Fig. 3c), respectively [51–53]. The basic structures and working principles of these three types of inchworm piezoelectric motors are elaborated in the following discussion.

3.2 Walker Inchworm Motor

The walker inchworm motor consists of one feeding module and two clamping modules. As shown in Fig. 3a, the feeding module and two clamping modules are all installed on the rotor, which rotate with the rotor during the operation process of the walker inchworm motor [51–53]. The stepping motion process of the walker inchworm motor is shown in Fig. 3a from Step (0) to Step (7), which are described as follows:

(1) The initial status of the walker inchworm motor.
(2) The clamping module at the right side runs and clamps the feeding module to the stator.
(3) The feeding module runs and pushes the upper clamping module and the rotor to rotate by an angle θ, anticlockwise.
(4) The upper clamping module runs and clamps the rotor to the stator.
(5) The clamping module at the right side is reset and releases the feeding module from the stator.
(6) The feeding module is reset and pulls the clamping module at the right side to rotate anticlockwise.
(7) The clamping module at the right side runs again and clamps the feeding module to the stator again.
(8) The upper clamping module is reset and releases the rotor from the stator. The walker inchworm motor returns back to the status in Step (1).

After the above operations from Step (1) to Step (7), the walker inchworm motor drives the rotor by an angle θ anticlockwise and returns back to the status in Step (1). If the above operations are repeated time by time, the walker inchworm motor can continually output angular displacements step by step. In addition, the backward rotary motions can be generated by adjusting the working sequences of the feeding module and two clamping modules.

3.3 Pusher Inchworm Motor

The pusher inchworm motor consists of one feeding module and two clamping modules. As shown in Fig. 3b, the feeding module and two clamping modules are all installed on the stator and do not rotate with the rotor during the operation process of the pusher inchworm motor [51–53]. The stepping motion process of the pusher inchworm motor is shown in Fig. 3b from Step (0) to Step (7), which are described as follows:

(1) The initial status of the pusher inchworm motor.
(2) The upper clamping module runs and clamps the rotor to the feeding module.
(3) The feeding module runs and pushes the upper clamping module and the rotor to rotate by an angle θ, anticlockwise.
(4) The clamping module at the right side runs and clamps the rotor to the stator.
(5) The upper clamping module is reset and releases the rotor from the feeding module.
(6) The feeding module is reset and pulls the upper clamping module to rotate clockwise.
(7) The upper clamping module runs again and clamps the rotor to the feeding module again.
(8) The clamping module at the right side is reset and releases the rotor from the stator. The pusher inchworm motor returns back to the status in Step (1).

After the above operations from Step (1) to Step (7), the pusher inchworm motor drives the rotor by an angle θ anticlockwise and returns back to the status in Step (1). If the above operations are repeated time by time, the pusher inchworm motor can continually output angular displacements step by step. In addition, the backward rotary motions can be

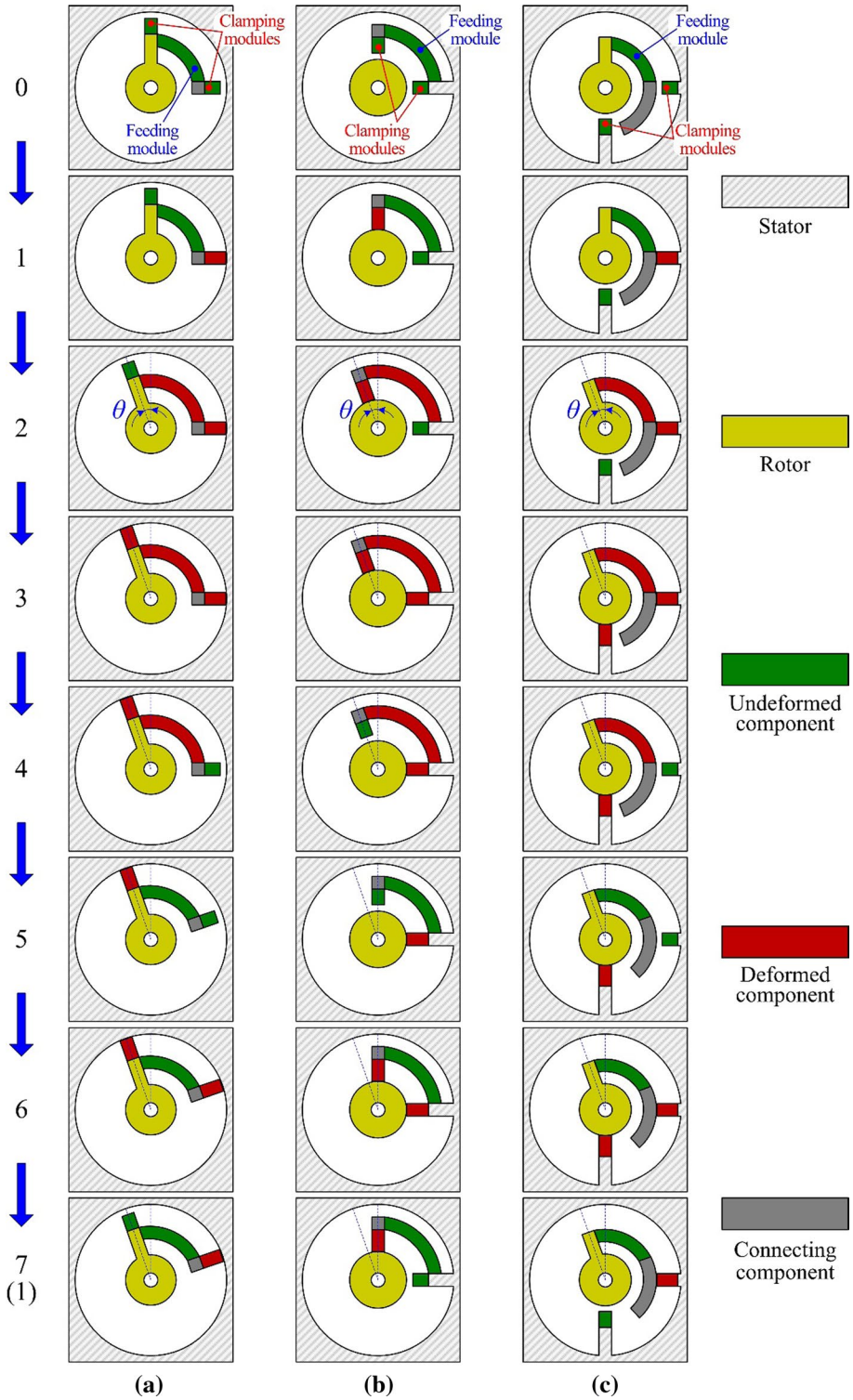

Fig. 3 Working principles of the inchworm motors. **a** Walker inchworm motor; **b** pusher inchworm motor; **c** hybrid inchworm motor

generated by adjusting the working sequences of the feeding module and two clamping modules.

3.4 Hybrid Inchworm Motor

The hybrid inchworm motor also consists of one feeding module and two clamping modules. As shown in Fig. 3c, the feeding module is installed on the rotor while the two clamping modules are installed on the stator [51–53].

Certainly, the positions of the feeding module and two clamping modules can also be exchanged. The module which is installed on the rotor rotates with it during the operation process of the hybrid inchworm motor and the module installed on the stator is relative static with the stator [51–53]. The stepping motion process of the hybrid inchworm motor is shown in Fig. 3c from Step (0) to Step (7), which are described as follows:

(1) The initial status of the hybrid inchworm motor.
(2) The clamping module at the right side runs and clamps the feeding module to the stator.
(3) The feeding module runs and pushes the rotor to rotate by an angle θ, anticlockwise.
(4) The lower clamping module runs and clamps the rotor to the stator.
(5) The clamping module at the right side is reset and releases the feeding module from the stator.
(6) The feeding module is reset and pulls the right part to rotate anticlockwise.
(7) The clamping module at the right side runs again and clamps the feeding module to the stator again.
(8) The lower clamping module is reset and releases the rotor from the stator. The hybrid inchworm motor returns back to the status in Step (1).

After the above operations from Step (1) to Step (7), the hybrid inchworm motor drives the rotor by an angle θ anticlockwise and returns back to the status in Step (1). If the above operations are repeated time by time, the hybrid inchworm motor can continually output angular displacements step by step. In addition, the backward rotary motions can be generated by adjusting the working sequences of the feeding module and two clamping modules.

4 Seal Piezoelectric Motors

4.1 Seal Motion Principle

The seal is a marine mammal with a contractible body and two pairs of feet. The body is elastic and can expand and contract. The hind feet have degenerated into fins without walking ability, while the fore feet can bend and assist crawling. As shown in Fig. 4, the crawling manner of the seal is another type of stepping motion, which is different from the inchworm type. The process is as follows: first, the seal is on the beach with the cumbersome body; second, it grips on the ground with the fore feet; third, it contracts the body and pulls forward the tail and the hind feet; fourthly, it releases the fore feet from the ground; lastly, it expands the body and pushes forward the fore feet and the head. After the above process, the seal moves forward one step on the beach and returns back to the initial status (the first step). Obviously, if the above process is repeated time after time, the seal can crawl with a long distance on the beach.

Inspired by the crawling mode of the seal, the seal-type bionic stepping piezoelectric motors are developed. As shown in Fig. 5, the seal piezoelectric motors are mainly composed of a feeding module to imitate the contractible body, a clamping module to imitate the fore feet with the crawling ability and a locking component to imitate the hind feet without crawling ability [54–56]. The feeding module is used to generate the driving angular displacements and the clamping module is employed to clamp or unclamp the rotor at the right time interval. The locking component is utilized to maintain the output thrust during the unclamping time interval of the clamping module. According to the relative position relationships among the feeding module, clamping module, and locking component, the seal piezoelectric motors can further be classified into three types, which are named walker seal motors (see Fig. 5a), pusher seal motors

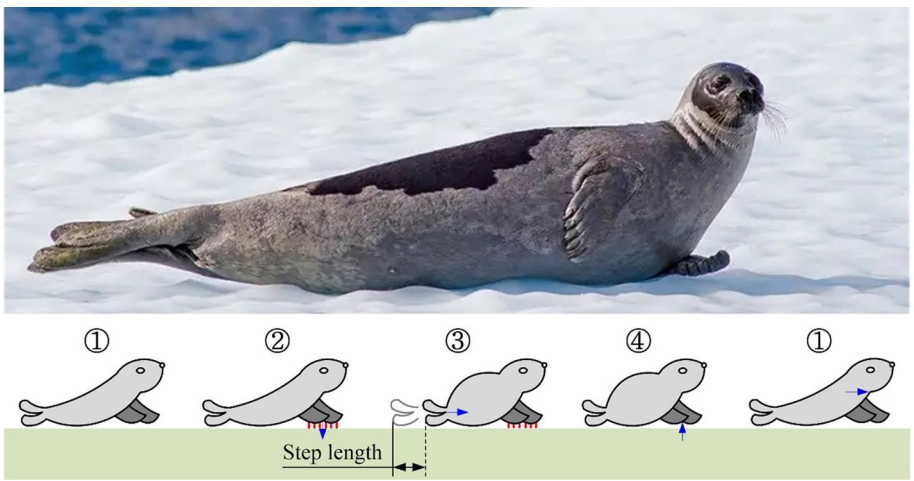

Fig. 4 Stepping motion of the seal

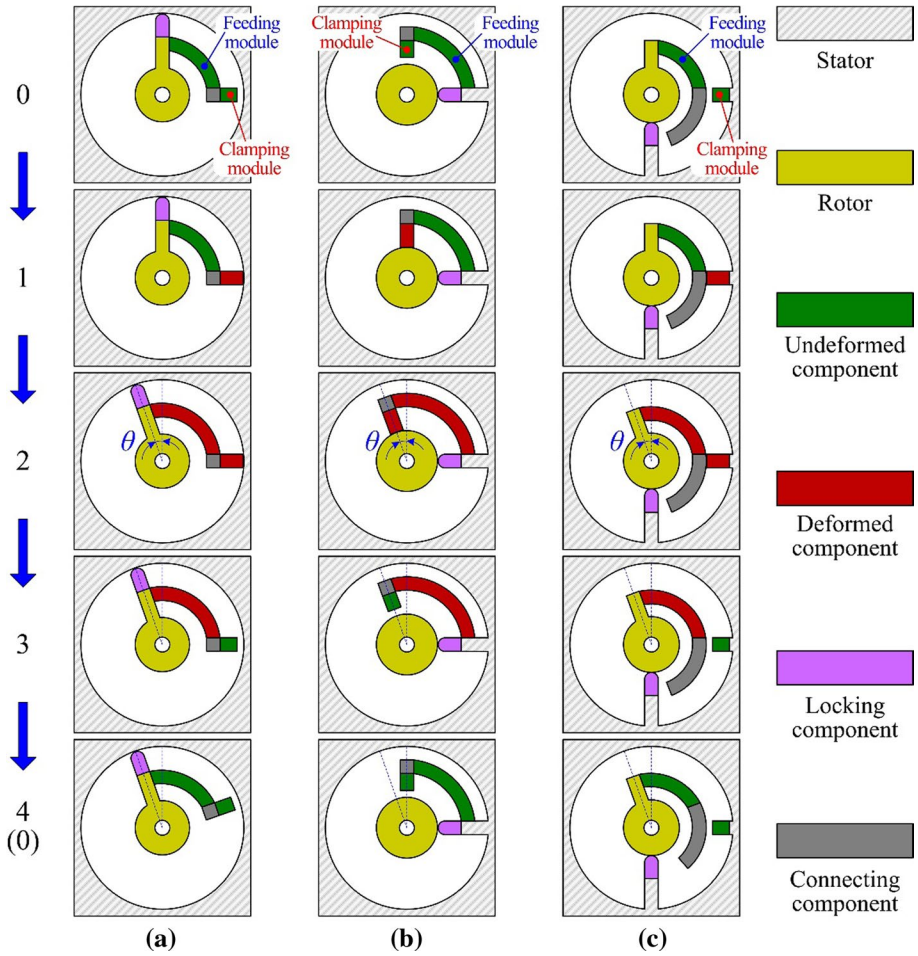

Fig. 5 Working principles of the seal motors. **a** Walker seal motor; **b** pusher seal motor; **c** hybrid seal motor

(see Fig. 5b), and hybrid seal motors (see Fig. 5c), respectively [54–56]. The basic structures and working principles of these three types of seal piezoelectric motors are elaborated in the following discussion.

4.2 Walker Seal Motor

The walker seal motor consists of one feeding module, one clamping module, and one locking component. As shown in Fig. 5a, the feeding module, the clamping module, and the locking component are all installed on the rotor and rotate with the rotor during the operation process of the walker seal motor [54–56]. The stepping motion process of the walker seal motor is shown in Fig. 5a from Step (0) to Step (4), which are described as follows:

(1) The initial status of the walker seal motor.
(2) The clamping module runs and clamps the feeding module to the stator.
(3) The feeding module runs and pushes the locking component and the rotor to rotate by an angle θ, anticlockwise.
(4) The clamping module is reset and releases the feeding module from the stator.
(5) The feeding module is reset and pulls the clamping module to rotate anticlockwise and the walker seal motor returns back to the status in Step (0).

After the above operations from Step (0) to Step (4), the walker seal motor drives the rotor by an angle θ anticlockwise and returns back to the status in Step (0). If the above operations are repeated time by time, the walker seal motor can continually output angular displacements step by step. The locking component can maintain the output thrust for the walker seal motor throughout the process. In addition, the backward rotary motions can be generated by adjusting the working sequences of the feeding module and the clamping module.

4.3 Pusher Seal Motor

The pusher seal motor consists of one feeding module, one clamping module, and one locking component. As shown in Fig. 5b, the feeding module, the clamping module, and the locking component are all installed on the stator and do

not rotate with the rotor during the operation process of the pusher seal motor [54–56]. The stepping motion process of the pusher seal motor is shown in Fig. 5b from Step (0) to Step (4), which are described as follows:

(1) The initial status of the pusher seal motor.
(2) The clamping module runs and clamps the rotor to the feeding module.
(3) The feeding module runs and pushes the clamping module and the rotor to rotate by an angle θ, anticlockwise.
(4) The clamping module is reset and releases the rotor from the feeding module.
(5) The feeding module is reset and pulls the clamping module to rotate clockwise and the pusher seal motor returns back to the status in Step (0).

After the above operations from Step (0) to Step (4), the pusher seal motor drives the rotor by an angle θ anticlockwise and returns back to the status in Step (0). If the above operations are repeated time by time, the pusher seal motor can continually output angular displacements step by step. The locking component can maintain the output thrust for the pusher seal motor throughout the process. In addition, the backward rotary motions can be generated by adjusting the working sequences of the feeding module and the clamping module.

4.4 Hybrid Seal Motor

The hybrid seal motor also consists of one feeding module, one clamping module, and one locking component. As shown in Fig. 5c, the feeding module is installed on the rotor while the clamping module and the locking component are both installed on the stator. Certainly, the positions of the feeding module, clamping module, and locking component can be exchanged. The module which is installed on the rotor rotates with the rotor during the operation process of the hybrid seal motor and the module which is installed on the stator is relative static with the stator [54–56]. The stepping motion process of the hybrid seal motor is shown in Fig. 5c from Step (0) to Step (4), which are described as follows:

(1) The initial status of the hybrid seal motor.
(2) The clamping module runs and clamps the feeding module to the stator.
(3) The feeding module runs and pushes the rotor to rotate by an angle θ, anticlockwise.
(4) The clamping module is reset and releases the feeding module from the stator.
(5) The feeding module is reset and pulls the right part to rotate anticlockwise and the hybrid seal motor returns back to the status in Step (0).

After the above operations from Step (0) to Step (4), the hybrid seal motor drives the rotor by an angle θ anticlockwise and returns back to the status in Step (0). If the above operations are repeated time by time, the hybrid seal motor can continually output angular displacements step by step. The locking component can maintain the output thrust for the hybrid seal motor throughout the process. In addition, the backward rotary motions can be generated by adjusting the working sequences of the feeding module and the clamping module.

5 Inertia Piezoelectric Motors

5.1 Inertia Motion Principle

IN nature, there are many examples that animals use inertia to achieve some goals. Dogs use inertia to shake off the water drops on hairs. Another more typical example is that the rhinoceros utilize inertia to assist their parturition. Due to the lack of external pulling force, it is difficult for the rhinoceros to deliver quickly. As shown in Fig. 6, the

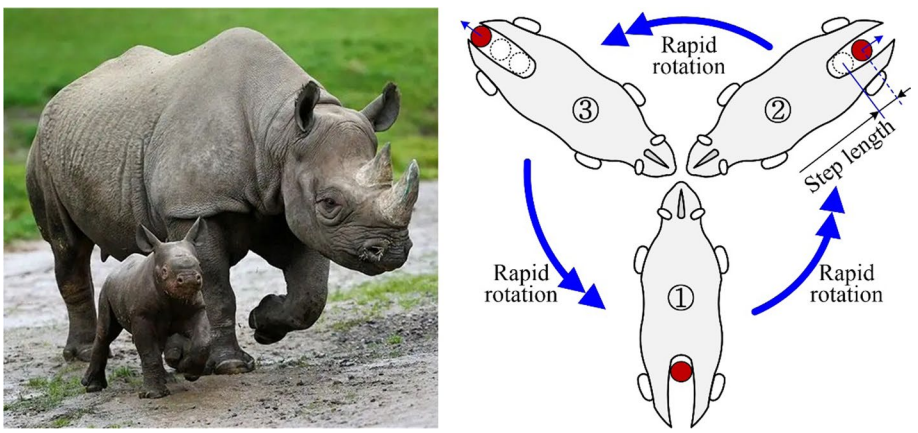

Fig. 6 Parturition with inertia force

rhinoceros rotates the body time after time to fling the hip in order to accelerate the parturition process. Under the action of the self-inertia, the cub can be flung out of the birth canal step by step. Finally, the rhinoceros cub is born successfully.

Imitating the parturition manner of the rhinoceros, the inertia-type bionic stepping piezoelectric motors are developed. As shown in Fig. 7, the inertia piezoelectric motors are mainly composed of one feeding module, one locking component, and one inertia mass [57–60]. The feeding module is used to generate the driving angular displacements. The locking component is employed to maintain the output thrust throughout the working process. The inertia mass is utilized to generate the inertia torque to drive the rotor. According to the relative position relationships among the feeding module, the locking component, and the inertia mass, the inertia piezoelectric motors can be classified into three types, which are named walker inertia motors (see Fig. 7a), pusher inertia motors (see Fig. 7b), and hybrid inertia motors (see Fig. 7c), respectively [57–60]. The basic structures and working principles of the three types of inertia piezoelectric motors are elaborated in the following discussion.

5.2 Walker Inertia Motor

The walker inertia motor, which is usually called impact type motor, consists of one feeding module, one locking component, and one inertia mass. As shown in Fig. 7a, the feeding module, the locking component, and the inertia mass are all installed on the rotor and rotated with the rotor during the operation process of the walker inertia motor [57–60]. The stepping motion process of the walker inertia motor is shown in Fig. 7a from Step (0) to Step (2), which are described as follows:

(1) The initial status of the walker inertia motor.
(2) The feeding module runs rapidly. Under the action of self-inertia, the inertia mass stays still and the rotor and the locking component are pushed rapidly to rotate by an angle θ, anticlockwise.
(3) The feeding module is reset slowly. Under the action of the locking component, the rotor and the locking component stay still and the inertia mass is pulled slowly to rotate anticlockwise. The walker inertia motor returns back to the status in Step (0).

After the above operations from Step (0) to Step (2), the walker inertia motor drives the rotor by an angle θ anticlockwise and returns back to the status in Step (0). If the above operations are repeated time by time, the walker inertia motor can continually output angular displacements step by step. The locking component can maintain the output thrust for the walker inertia motor throughout the process. In addition, the backward rotary motions can be generated by exchanging the rapid functional step and the slow functional step of the feeding module.

5.3 Pusher Inertia Motor

The pusher inertia motor, which is usually called stick–slip type motor, consists of one feeding module, one locking component, and one inertia mass. As shown in Fig. 7b, the feeding module, the locking component, and the inertia mass are all installed on the stator and do not rotate with the rotor during the operation process of the pusher inertia motor [57–60]. The stepping motion process of the pusher inertia motor is shown in Fig. 7b from Step (0) to Step (2), which are described as follows:

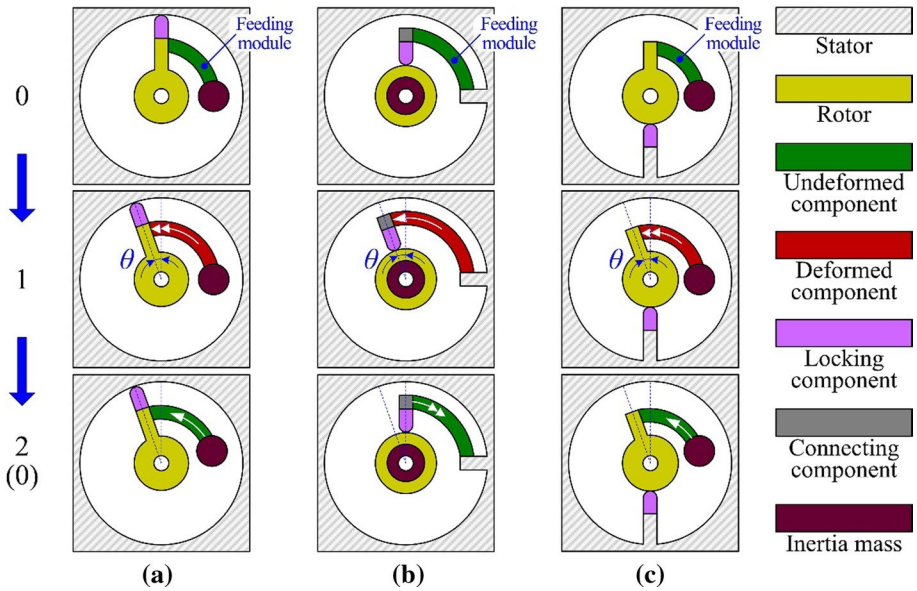

Fig. 7 Working principles of the inertia motors. **a** Walker inertia motor (Impact type motor); **b** pusher inertia motor (stick–slip type motor); **c** hybrid inertia motor

(1) The initial status of the pusher inertia motor.
(2) The feeding module runs slowly. Under the action of the locking component, the rotor and the inertia mass are pushed slowly to rotate by an angle θ, anticlockwise.
(3) The feeding module is reset rapidly. Under the action of inertia of the inertia mass, the rotor and inertia mass stay still and the locking component is pulled rapidly to rotate clockwise. The pusher inertia motor returns back to the status in Step (0).

After the above operations from Step (0) to Step (2), the pusher inertia motor drives the rotor by an angle θ anticlockwise and returns back to the status in Step (0). If the above operations are repeated time by time, the pusher inertia motor can continually output angular displacements step by step. The locking component can maintain the output thrust for the pusher inertia motor throughout the process. In addition, the backward rotary motions can be generated by exchanging the rapid functional step and the slow functional step of the feeding module.

5.4 Hybrid Inertia Motor

The hybrid inertia motor also consists of one feeding module, one locking component and one inertia mass. As shown in Fig. 7c, the feeding module and the inertia mass are both installed on the rotor while the locking component is installed on the stator [57–60]. The positions of the feeding module, locking component, and inertia mass can be exchanged. The module installed on the rotor rotates with the rotor during the operation process of the hybrid inertia motor, while the module installed on the stator is relative static with the stator. The stepping motion process of the hybrid inertia motor is shown in Fig. 7c from Step (0) to Step (2), which are described as follows:

(1) The initial status of the hybrid inertia motor.
(2) The feeding module runs rapidly. Under the action of self-inertia, inertia mass stays still and the rotor is pushed rapidly to rotate by an angle θ, anticlockwise.
(3) The feeding module is reset slowly. Under the action of the locking component, the rotor stays still and the inertia mass is pulled slowly to rotate anticlockwise. The hybrid inertia motor returns back to the status in Step (0).

After the above operations from Step (0) to Step (2), the hybrid inertia motor drives the rotor by an angle θ anticlockwise and returns back to the status in Step (0). If the above operations are repeated time by time, the hybrid inertia motor can continually output angular displacements step by step. The locking component can maintain the output thrust for the hybrid inertia motor throughout the process. In addition, the backward rotary motions can be generated by exchanging the rapid functional step and the slow functional step of the feeding module.

6 Characteristics of Stepping Piezoelectric Motors

By virtue of the bionic stepping principles, the piezoelectric motor can accumulate small displacements from the piezoelectric materials step by step and generate a long-range working stroke. Consequently, the piezoelectric motors completely liberate themselves from the small deformations and inherit the main advantages of piezoelectric materials as well. The work range of stepping piezoelectric motors can reach several radians, or even without limit, and the resolution can reach microradian. The inchworm motors, seal motors, and inertia motors are the three types of most commonly used bionic stepping piezoelectric motors. In Table 1, the performance data of typical stepping piezoelectric motors are summarized.

In terms of the configurations, the inchworm motor contains one feeding module and two clamping modules. If one of these two clamping modules is replaced by a locking component, the inchworm motor can be transformed into a seal motor. Therefore, the seal motor contains one feeding module, one clamping module, and one locking component. If the other clamping module is further replaced by an inertia mass, the seal motor is transformed into an inertia motor. Therefore, the inertia motor contains one feeding module, one locking component, and one inertia mass. These are the transformational relations among the three types of bionic stepping piezoelectric motors. Moreover, the characteristics of the three types of motors are compared in Table 2.

The clamping module can provide a large clamping force during the stepping motion. However, it has a complicated structure and requires additional control and enough time response during the clamping process. Moreover, the contact and separation of the clamping module cause vibrations and

Table 1 Performance of stepping piezoelectric motors

Item\Type	Inchworm motor [50]	Seal motor [54]	Inertia motor [59]
Stroke	4 mm	19 mm	14 mm
Resolution	31.5 nm	25.9 nm	13 nm
Structure	$165\times150\times15$ mm^3	$90\times45\times14.5$ mm^3	$30\times11\times11$ mm^3
Oscillation	0.74 μm	0.63 μm	N/A
Capacity	123.5 N	3.2 N	0.21 N
Velocity	0.25 mm s^{-1}	0.34 mm s^{-1}	31.7 mm s^{-1}

Table 2 Characteristics of stepping piezoelectric motors

Item\Type	Inchworm motor	Seal motor	Inertia motor
Stroke	Long	Long	Long
Resolution	High	High	High
Structure	Oversized	Intermediate	Compact
Oscillation	Large	Intermediate	Small
Capacity	Large	Intermediate	Small
Velocity	Slow	Intermediate	Fast
Control	Complicated	Intermediate	Simple

motion errors in the rotor. Therefore, the inchworm motors composed of one feeding module and two clamping modules show large load capacity, whereas they have oversized structure, large oscillation, slow velocity, and complicated control system [61–72]. In contrast, the inertia motors, which are composed of one feeding module, one locking component, and one inertia mass, have compact structure, small oscillation, fast velocity, and a simple control system, while the load capacity is small [73–82]. In addition, due to the intrinsic limitation of the inertia principle, there is rollback motion at every step of the inertia motor. Large preload force of the rotor and the large mass of the inertia block can reduce the rollback motion and increase the load capacity of the inertia motor. As for the seal motors composed of one feeding module, one clamping module and one locking component, the properties of the structure, oscillation, and velocity as well as the complexity of control system are at an intermediate level between those of the inchworm motors and inertia motors [83–100].

According to the relative position relationships among the main structure modules, each of the inchworm motor, seal motor, and inertia motor can be classified into walker type, pusher type, and hybrid type. For the walker motor, all the functional modules are installed on the rotor. Namely, the walker motor possesses a stator with simple structures and a rotor with complex structures [61–72]. For the pusher motor, all the functional modules are installed on the stator. Therefore, the pusher motor has a stator with a complex structure and a rotor with a simple structure [73–82]. For the hybrid motor, the functional modules are installed on both the stator and the rotor. Therefore, the hybrid motor possesses a moderate stator and a moderate rotor [73–82]. Generally, the walker motor has large capacity. Because the long radius of the big volume rotor contributes to the large driving torque [61–68]. If the capability to output many revolutions of the motor is required, the pusher motor is the optimal choice, as there is no electric module on the rotor. In addition, the pusher motor is provided with a high speed due to the light weight of the rotor [61–82]. Clearly, the characteristics of the hybrid motor are at an intermediate level between those of the walker motor and the pusher motor [95–100].

7 Conclusions

In this work, the bionic stepping motors driven by piezoelectric materials are comprehensively reviewed. The characteristics of three important bionic stepping piezoelectric motors are elaborated, including the inchworm motors, seal motors, and inertia motors, which all present high motion resolution and long working stroke. The mutual transformation relationships among the three types of motors by replacing certain components are elaborated especially. The inchworm motors composed of one feeding module and two clamping modules show large load capacity, whereas they have oversized structure, large oscillation, slow velocity, and complicated control system. In contrast, the inertia motors, composed of one feeding module, one locking component, and one inertia mass, have a compact structure, small oscillation, fast velocity, and a simple control system, while the load capacity is small. As for the seal motors composed of one feeding module, one clamping module, and one locking component, the properties of the structure, oscillation and velocity, as well as the complexity of the control system are at an intermediate level between those of the inchworm motors and inertia motors. Moreover, each of the inchworm motors, seal motors and inertia motors can further be classified into walker type, pusher type, and hybrid type, according to the relative position relationships among the main structure modules. The walker type possesses large capacity, while its velocity is smaller than the pusher type. The characteristics of the hybrid type are intermediate as compared to the walker type, and pusher type. In summary, the structures, principles, classifications, correlations, and performance of various types of bionic stepping piezoelectric motors are elaborated and reviewed. The work is beneficial for researchers and engineers to investigate the existing piezoelectric motors and to explore novel driving principles and methods for better engineering applications.

Future research directions are suggested as follows:

(1) The clamping components need to be improved to reduce the vibration of the rotor during the clamping movement.
(2) Structure optimization, lightweight material, and advanced process can profit the compact volume, stable operation, and performance improvement of the stepping piezoelectric motors.
(3) It is of significance to develop piezoelectric motors with multiple degrees of freedom and multiple stepping principles.
(4) New stepping principles and novel driving methods should continue to be explored to elevate the performance of piezoelectric motors.

Acknowledgements This work was supported by the Natural Science Foundation of Jilin Province (Grant No. 20220101216JC) and the Talent Introduction Fund of Jilin University (Grant No. 451210330007).

Funding Natural Science Foundation of Jilin Province, 20220101216JC, Shupeng Wang, Talent Introduction Fund of Jilin University, 451210330007, Shupeng Wang.

Data Availability Statement The datasets generated during and/or analyzed during the current study are available from the corresponding author on reasonable request.

Declarations

Conflict of interest On behalf of all authors, the corresponding author states that there is no conflict of interest.

References

1. Lin, F. J., Hung, Y. C., & Chen, S. Y. (2009). FPGA-based computed force control system using elman neural network for linear ultrasonic motor. *IEEE Transactions on Industrial Electronics, 56*(4), 1238–1253. https://doi.org/10.1109/TIE.2008.2007040
2. Cheng, L., Liu, W. C., Hou, Z. G., Yu, J. Z., & Tan, M. (2015). Neural-network-based nonlinear model predictive control for piezoelectric actuators. *IEEE Transactions on Industrial Electronics, 62*(12), 7717–7727. https://doi.org/10.1109/TIE.2015.2455026
3. Wang, L., Wang, H. R., & Cheng, T. H. (2022). Design and performance of a compact stick-slip type piezoelectric actuator based on right triangle flexible stator. *Smart Materials and Structures, 31*(5), 055013. https://doi.org/10.1088/1361-665X/ac6206
4. Kang, B. W., & Kim, J. (2013). Design, fabrication, and evaluation of stepper motors based on the piezoelectric torsional actuator. *IEEE/ASME Transactions on Mechatronics, 18*(6), 1850–1854. https://doi.org/10.1109/TMECH.2013.2269171
5. Wang, S. P., Rong, W. B., Wang, L. F., Pei, Z. C., & Sun, L. N. (2017). Design, analysis and experimental performance of a bionic piezoelectric rotary actuator. *Journal of Bionic Engineering, 14*, 348–355. https://doi.org/10.1016/S1672-6529(16)60403-1
6. Wang, S. P., Rong, W. B., Wang, L. F., Pei, Z. C., & Sun, L. N. (2017). Design, analysis and experimental performance of a novel stick-slip type piezoelectric rotary actuator based on variable force couple driving. *Smart Materials and Structures, 26*(5), 055005. https://doi.org/10.1088/1361-665X/aa64c3
7. Henke, B., Sawodny, O., & Neumann, R. (2015). Distributed parameter modeling of flexible ball screw drives using ritz series discretization. *IEEE/ASME Transactions on Mechatronics, 20*(3), 1226–1235. https://doi.org/10.1109/TMECH.2014.2333775
8. Hwang, D., Ihn, Y. S., & Kim, K. (2018). Compact modular cycloidal motor with embedded shape memory alloy wires. *IEEE Transactions on Industrial Electronics, 65*(5), 4028–4038. https://doi.org/10.1109/TIE.2017.2764839
9. Mirvakili, S. M., & Hunter, I. W. (2018). Artificial muscles: Mechanisms, applications, and challenges. *Advanced Materials, 30*(6), 1704407. https://doi.org/10.1002/adma.201704407
10. Lallart, M., Richard, C., Sukwisut, P., Petit, L., Guyomar, D., & Muensit, N. (2012). Electrostrictive bending actuators: Modeling and experimental investigation. *Sensors and Actuators A: Physical, 179*, 169–177. https://doi.org/10.1016/j.sna.2012.02.023
11. Santapuri, S., Scheidler, J. J., & Dapino, M. J. (2015). Two-dimensional dynamic model for composite laminates with embedded magnetostrictive materials. *Composite Structures, 132*, 737–745. https://doi.org/10.1016/j.compstruct.2015.04.062
12. Lv, Q. B., Yao, Z. Y., Jin, Y. Q., & Liu, B. (2022). Wear evaluation model of a linear piezoelectric ultrasonic motor considering temperature effect. *Ultrasonics, 126*, 106822. https://doi.org/10.1016/j.ultras.2022.106822
13. Lucinskis, R., Mazeika, D., & Bansevicius, R. (2018). Investigation of oscillations of piezoelectric actuators with multi-directional polarization. *Mechanical Systems and Signal Processing, 99*, 450–458. https://doi.org/10.1016/j.ymssp.2017.06.036
14. Yildirim, Y. A., Toprak, A., & Tigli, O. (2017). Piezoelectric membrane actuators for micropump applications using PVDF-TrFE. *Journal of Microelectromechanical Systems, 27*(1), 86–94. https://doi.org/10.1109/JMEMS.2017.2773090
15. Shafik, A., & Mrad, R. B. (2016). Piezoelectric motor technology: A review. In: Ru, C., Liu, X., & Sun, Y (Eds.), *Nanopositioning Technologies* (pp. 33–59). Springer, Cham. https://doi.org/10.1007/978-3-319-23853-1_2
16. Zhu, C., Chu, X. C., Yuan, S. M., Zhong, Z. J., Zhao, Y. Q., & Gao, S. N. (2016). Development of an ultrasonic linear motor with ultra-positioning capability and four driving feet. *Ultrasonics, 72*, 66–72. https://doi.org/10.1016/j.ultras.2016.07.010
17. Han, S., Li, Z., Xu, Y. L., & Yang, X. F. (2022). Design and experimental evaluation of an inchworm motor driven by bender-type piezoelectric actuators. *Smart Materials and Structures, 31*(11), 115004. https://doi.org/10.1088/1361-665X/ac93d2
18. Poikselkä, K., Leinonen, M., Palosaari, J., Vallivaara, I., Röning, J., & Juuti, J. (2017). Novel genetically optimised high-displacement piezoelectric actuator with efficient use of active material. *Smart Materials and Structures, 26*(9), 095022. https://doi.org/10.1088/1361-665X/aa770a
19. Li, J. P., Zhou, X. Q., Zhao, H. W., Shao, M. K., Li, N., Zhang, S. Z., & Du, Y. M. (2016). Development of a novel parasitic-type piezoelectric actuator. *IEEE/ASME Transactions on Mechatronics, 22*(1), 541–550. https://doi.org/10.1109/TMECH.2016.2604242
20. Esteves, G., Fancher, C. M., Röhrig, S., Maier, G. A., Jones, J. L., & Deluca, M. (2017). Electric-field-induced structural changes in multilayer piezoelectric actuators during electrical and mechanical loading. *Acta Materialia, 132*, 96–105. https://doi.org/10.1016/j.actamat.2017.04.014
21. Kaufmann, P., Röhrig, S., Supancic, P., & Deluca, M. (2017). Influence of ferroelectric domain texture on the performance of multilayer piezoelectric actuators. *Journal of the European Ceramic Society, 37*(5), 2039–2046. https://doi.org/10.1016/j.jeurceramsoc.2016.12.029
22. Zhang, Y., Zhang, W. J., Hesselbach, J., & Kerle, H. (2006). Development of a two-degree-of-freedom piezoelectric rotary-linear actuator with high driving force and unlimited linear movement. *Review of Scientific Instruments, 77*(3), 035112. https://doi.org/10.1063/1.2185500

23. Ho, S. T., & Jan, S. J. (2016). A piezoelectric motor for precision positioning applications. *Precision Engineering, 43*, 285–293. https://doi.org/10.1016/j.precisioneng.2015.08.007
24. Lee, J. W., Li, Y. C., Chen, K. S., & Liu, Y. H. (2016). Design and control of a cascaded piezoelectric actuated two-degrees-of-freedom positioning compliant stage. *Precision Engineering, 45*, 374–386. https://doi.org/10.1016/j.precisioneng.2016.03.015
25. Ham, Y. B., Seo, W. S., Cho, W. Y., Yun, D. W., Park, J. H., & Yun, S. N. (2009). Development of a piezoelectric pump using hinge-lever amplification mechanism. *Journal of Electroceramics, 23*(2), 346–350. https://doi.org/10.1007/s10832-008-9461-y
26. Na, T. W., Choi, J. H., Jung, J. Y., Kim, H. G., Han, J. H., Park, K. C., & Oh, I. K. (2016). Compact piezoelectric tripod manipulator based on a reverse bridge-type amplification mechanism. *Smart Materials and Structures, 25*(9), 095028. https://doi.org/10.1088/0964-1726/25/9/095028
27. Chen, W. L., Zhang, X. M., Li, H., Wei, J. Y., & Fatikow, S. (2017). Nonlinear analysis and optimal design of a novel piezoelectric-driven compliant microgripper. *Mechanism and Machine Theory, 118*, 32–52. https://doi.org/10.1016/j.mechmachtheory.2017.07.011
28. Chen, C. M., Hsu, Y. C., & Fung, R. F. (2012). System identification of a Scott-Russell amplifying mechanism with offset driven by a piezoelectric actuator. *Applied Mathematical Modelling, 36*(6), 2788–2802. https://doi.org/10.1016/j.apm.2011.09.064
29. Tian, Y. L., Shirinzadeh, B., Zhang, D. W., & Alici, G. (2009). Development and dynamic modelling of a flexure-based Scott-Russell mechanism for nano-manipulation. *Mechanical Systems and Signal Processing, 23*(3), 957–978. https://doi.org/10.1016/j.ymssp.2008.06.007
30. Rios, S. A., & Fleming, A. J. (2015). Design of a charge drive for reducing hysteresis in a piezoelectric bimorph actuator. *IEEE/ASME Transactions on Mechatronics, 21*(1), 51–54. https://doi.org/10.1109/TMECH.2015.2483739
31. Wang, H. R., Hu, M., & Li, Z. Q. (2016). Modelling and analysis of circular bimorph piezoelectric actuator for deformable mirror. *Applied Mathematics and Mechanics, 37*(5), 639–646. https://doi.org/10.1007/s10483-016-2077-8
32. Yong, Y. K., & Leang, K. K. (2016). Mechanical design of high-speed nanopositioning systems. In: Ru, C., Liu, X., Sun, & Y. (Eds.) *Nanopositioning Technologies* (pp. 61–121). Springer, Cham. https://doi.org/10.1007/978-3-319-23853-1_3
33. Nam, J., Oh, H., & Jang, G. (2016). Externally leveraged resonant piezoelectric actuator with fast response time for smart devices. *IEEE/ASME Transactions on Mechatronics, 21*(6), 2764–2772. https://doi.org/10.1109/TMECH.2016.2590564
34. Belly, C., & Charon, W. (2012). Benefits of amplification in an inertial stepping motor. *Mechatronics, 22*(2), 177–183. https://doi.org/10.1016/j.mechatronics.2012.01.006
35. Salisbury, S. P., Waechter, D. F., Mrad, R. B., Prasad, S. E., Blacow, R. G., & Yan, B. (2006). Design considerations for complementary inchworm actuators. *IEEE/ASME Transactions on Mechatronics, 11*(3), 265–272. https://doi.org/10.1109/TMECH.2006.875565
36. Yokozawa, H., & Morita, T. (2015). Wireguide driving actuator using resonant-type smooth impact drive mechanism. *Sensors and Actuators A: Physical, 230*, 40–44. https://doi.org/10.1016/j.sna.2015.04.012
37. Cera, M., Cirelli, M., Colaiacovo, L., & Valentini, P. P. (2022). Second-order approximation pseudo-rigid model of circular arc flexure hinge. *Mechanism and Machine Theory, 175*, 104963. https://doi.org/10.1016/j.mechmachtheory.2022.104963
38. Harfensteller, F., Henning, S., Zentner, L., & Husung, S. (2022). Modeling of corner-filleted flexure hinges under various loads. *Mechanism and Machine Theory, 175*, 104937. https://doi.org/10.1016/j.mechmachtheory.2022.104937
39. Liu, X. H., Gao, L., Wu, Y., Song, H. R., & He, Y. (2022). Micro-displacement amplifier of giant magnetostrictive actuator using flexure hinges. *Journal of Magnetism and Magnetic Materials, 556*, 169415. https://doi.org/10.1016/j.jmmm.2022.169415
40. Geva, K., Kahmann, H., Schlegel, C., & Kumme, R. (2022). Measurement uncertainty analysis of a measurement flexure hinge in a torque standard machine. *Journal of Sensors and Sensor Systems, 11*(2), 201–209. https://doi.org/10.5194/jsss-11-201-2022
41. Cammarata, A., Maddìo, P. D., Sinatra, R., Rossi, A., & Belfiore, N. P. (2022). Dynamic model of a conjugate-surface flexure hinge considering impacts between cylinders. *Micromachines, 13*(6), 957. https://doi.org/10.3390/mi13060957
42. Chen, F. X., Gao, Y. Z., Dong, W., & Du, Z. J. (2020). Design and control of a passive compliant piezo-actuated micro-gripper with hybrid flexure hinges. *IEEE Transactions on Industrial Electronics, 68*(11), 11168–11177. https://doi.org/10.1109/TIE.2020.3032921
43. Kim, I., Kim, Y. S., & Park, E. C. (2009). Sliding mode control of the inchworm displacement with hysteresis compensation. *International Journal of Precision Engineering and Manufacturing, 10*(3), 43–49. https://doi.org/10.1007/s12541-009-0046-8
44. Li, J. P., Zhao, H. W., Shao, M. K., Zhou, X. Q., Huang, H., & Fan, Z. Q. (2014). Design and experiment performances of an inchworm type rotary actuator. *Review of Scientific Instruments, 85*(8), 085004. https://doi.org/10.1063/1.4892998
45. Kato, H., Hayakawa, K., Torii, A., & Ueda, A. (2000). XYΘ actuators using piezoelectric and electromagnetic actuators. *Electrical Engineering in Japan, 131*(4), 44–51. https://doi.org/10.1002/(SICI)1520-6416(200006)131:4%3c44::AID-EEJ6%3e3.0.CO;2-R
46. Yan, S. Z., Zhang, F. X., Qin, Z., & Wen, S. Z. (2005). A 3-DOFs mobile robot driven by a piezoelectric actuator. *Smart Materials and Structures, 15*(1), N7–N13. https://doi.org/10.1088/0964-1726/15/1/N02
47. Wen, J. M., Ma, J. J., Zeng, P., Cheng, G. M., & Zhang, Z. H. (2013). A new inertial piezoelectric rotary actuator based on changing the normal pressure. *Microsystem Technologies, 19*(2), 277–283. https://doi.org/10.1007/s00542-012-1684-9
48. Zeng, P., Wen, J., Cheng, G., Wu, B., & Yang, Z. (2006). Research on novel inertial piezoelectric actuator. *Optics and Precision Engineering, 14*(4), 623–627.
49. Wang, S. P., Rong, W. B., Wang, L. F., Pei, Z. C., & Sun, L. N. (2018). A novel inchworm type piezoelectric rotary actuator with large output torque: Design, analysis and experimental performance. *Precision Engineering, 51*, 545–551. https://doi.org/10.1016/j.precisioneng.2017.10.010
50. Wang, S. P., Zhang, Z. H., Ren, L. Q., Zhao, H. W., Liang, Y. H., & Zhu, B. (2015). Design and driving characteristics of a novel 'pusher' type piezoelectric actuator. *Smart Materials and Structures, 25*(1), 015005. https://doi.org/10.1088/0964-1726/25/1/015005
51. Oh, C. H., Choi, J. H., Nam, H. J., Bu, J. U., & Kim, S. H. (2010). Ultra-compact, zero-power magnetic latching piezoelectric inchworm motor with integrated position sensor. *Sensors and Actuators A: Physical, 158*(2), 306–312. https://doi.org/10.1016/j.sna.2010.01.022
52. Li, J. P., Zhao, H. W., Qu, X. T., Qu, H., Zhou, X. Q., Fan, Z. Q., Ma, Z. C., & Fu, H. S. (2015). Development of a compact 2-DOF precision piezoelectric positioning platform based on inchworm principle. *Sensors and Actuators A: Physical, 222*, 87–95. https://doi.org/10.1016/j.sna.2014.12.001
53. Wang, S. P., Rong, W. B., Wang, L. F., Xie, H., Sun, L. N., & Mills, J. K. (2019). A survey of piezoelectric actuators with long working stroke in recent years: Classifications, principles,

connections and distinctions. *Mechanical Systems and Signal Processing, 123*, 591–605. https://doi.org/10.1016/j.ymssp.2019.01.033
54. Wang, S. P., Rong, W. B., Wang, L. F., Pei, Z. C., & Sun, L. N. (2018). Novel design, analytical and experimental studies of a piezoelectric ultrasonic linear actuator based on binate feet driving. *Journal of Intelligent Material Systems and Structures, 29*(5), 787–799. https://doi.org/10.1177/1045389X17721043
55. Furutani, K., & Kawagoe, K. (2010). Influence of slope angle and traction load on performance of azarashi (seal) mechanism with one degree of freedom. *IEEJ Transactions on Electrical and Electronic Engineering, 5*(2), 181–187. https://doi.org/10.1002/tee.20515
56. Furutani, K. (2010). Performance of AZARASHI (Seal) positioning mechanism with friction control by inertial force. *International Journal of the Japan Society for Precision Engineering, 76*, 679–683.
57. Neuman, J., Nováček, Z., Pavera, M., Zlámal, J., Kalousek, R., Spousta, J., Dittrichová, L., & Šikola, T. (2015). Experimental optimization of power-function-shaped drive pulse for stick-slip piezo actuators. *Precision Engineering, 42*, 187–194. https://doi.org/10.1016/j.precisioneng.2015.04.016
58. Cheng, L., Liu, W. C., Yang, C. G., Huang, T. W., Hou, Z. G., & Tan, M. (2017). A neural-network-based controller for piezoelectric-actuated stick–slip devices. *IEEE Transactions on Industrial Electronics, 65*(3), 2598–2607. https://doi.org/10.1109/TIE.2017.2740826
59. Song, X., Wang, H. Q., Zhang, Y. K., Liu, W. M., Liu, L., & Peng, Y. X. (2020). A miniaturized dual-slider linear actuator using electrostatic adhesion and inertia drive. *Actuators, 9*(4), 114. https://doi.org/10.3390/act9040114
60. Peng, Y. X., Peng, Y. L., Gu, X. Y., Wang, J., & Yu, H. Y. (2015). A review of long range piezoelectric motors using frequency leveraged method. *Sensors and Actuators A: Physical, 235*, 240–255. https://doi.org/10.1016/j.sna.2015.10.015
61. Mohammad, T., & Salisbury, S. P. (2014). Design and assessment of a Z-axis precision positioning stage with centimeter range based on a piezoworm motor. *IEEE/ASME Transactions on Mechatronics, 20*(5), 2021–2030. https://doi.org/10.1109/TMECH.2014.2360644
62. Deng, J., Zhang, S. J., Li, Y. Q., Ma, X. F., Gao, X., Xie, H., & Liu, Y. X. (2022). Development and experiment evaluation of a compact inchworm piezoelectric actuator using three-jaw type clamping mechanism. *Smart Materials and Structures, 31*(4), 045020. https://doi.org/10.1088/1361-665X/ac59da
63. Koh, J. S., & Cho, K. J. (2012). Omega-shaped inchworm-inspired crawling robot with large-index-and-pitch (LIP) SMA spring actuators. *IEEE/ASME Transactions On Mechatronics, 18*(2), 419–429. https://doi.org/10.1109/TMECH.2012.2211033
64. Tahmasebipour, M., & Sangchap, M. (2019). A novel high performance integrated two-axis inchworm piezoelectric motor. *Smart Materials and Structures, 29*(1), 015034. https://doi.org/10.1088/1361-665X/ab545e
65. Shao, S. B., Song, S. Y., Liu, K. Y., & Xu, M. L. (2019). A piezo-driven rotary inchworm actuator featured with simple structure and high output torque. *International Journal of Applied Electromagnetics and Mechanics, 59*(1), 317–325. https://doi.org/10.3233/JAE-171177
66. Sun, T. T., Wang, Y., & Yan, P. (2021). Analysis and variable step control of a bidirectional complementary-type inchworm actuator. *Smart Materials and Structures, 30*(4), 045019. https://doi.org/10.1088/1361-665X/abe33a
67. Ma, X. F., Liu, Y. X., Deng, J., Gao, X., & Cheng, J. F. (2023). A compact inchworm piezoelectric actuator with high speed: Design, modeling, and experimental evaluation. *Mechanical Systems and Signal Processing, 184*, 109704. https://doi.org/10.1016/j.ymssp.2022.109704
68. Ling, J., Chen, L., Feng, Z., & Zhu, Y. C. (2022). Development and test of a high speed pusher-type inchworm piezoelectric actuator with asymmetric driving and clamping configuration. *Mechanism and Machine Theory, 176*, 104997. https://doi.org/10.1016/j.mechmachtheory.2022.104997
69. Ghodsi, M., Mohammadzaheri, M., Soltani, P., & Ziaifar, H. (2022). A new active anti-vibration system using a magneto-strictive bimetal actuator. *Journal of Magnetism and Magnetic Materials, 557*, 169463. https://doi.org/10.1016/j.jmmm.2022.169463
70. Sun, T. T., & Yan, P. (2022). A novel high-speed bi-directional piezoelectric inchworm actuator based on flexible supported baffles. *Smart Materials and Structures, 31*(9), 095014. https://doi.org/10.1088/1361-665X/ac7dce
71. Shao, S. B., Song, S. Y., Shao, Y., & Xu, M. L. (2022). Long-range piezoelectric actuator with large load capacity using inchworm and stick-slip driving principles. *Precision Engineering, 75*, 167–179. https://doi.org/10.1016/j.precisioneng.2022.02.007
72. Vo, T. V. K., Lubecki, T. M., Chow, W. T., Gupta, A., & Li, K. H. H. (2021). Large-scale piezoelectric-based systems for more electric aircraft applications. *Micromachines, 12*(2), 140. https://doi.org/10.3390/mi12020140
73. Wang, F. J., Zhao, X. L., Huo, Z. C., Shi, B. C., Tian, Y. L., & Zhang, D. W. (2022). A novel large stepping-stroke actuator based on the bridge-type mechanism with asymmetric stiffness. *Mechanical Systems and Signal Processing, 179*, 109317. https://doi.org/10.1016/j.ymssp.2022.109317
74. Bian, L., Li, Z. M., Qi, X. D., Sun, Y., Jiang, G. C., Zhao, B., Yang, B., & Dong, S. X. (2022). Low-temperature sintered PMnS–PZT multilayer-ceramic for nano-step piezomotor application. *Sensors and Actuators A: Physical, 345*, 113812. https://doi.org/10.1016/j.sna.2022.113812
75. Yun, H., Kong, D. Q., & Aoyagi, M. (2022). Development of a multi-drive-mode piezoelectric linear actuator with parallel-arrangement dual stator. *Precision Engineering, 77*, 127–140. https://doi.org/10.1016/j.precisioneng.2022.05.014
76. Deng, J., Liu, Y. X., Li, J., Zhang, S. J., & Li, K. (2022). Displacement linearity improving method of stepping piezoelectric platform based on leg wagging mechanism. *IEEE Transactions on Industrial Electronics, 69*(6), 6429–6432. https://doi.org/10.1109/TIE.2021.3094477
77. Li, J. P., Huang, H., & Morita, T. (2019). Stepping piezoelectric actuators with large working stroke for nano-positioning systems: A review. *Sensors and Actuators A: Physical, 292*, 39–51. https://doi.org/10.1016/j.sna.2019.04.006
78. Pu, Y. X., Zhou, H. L., & Meng, Z. (2019). Multi-channel adaptive active vibration control of piezoelectric smart plate with online secondary path modelling using PZT patches. *Mechanical Systems and Signal Processing, 120*, 166–179. https://doi.org/10.1016/j.ymssp.2018.10.019
79. Hunstig, M. (2017). Piezoelectric inertia motors—A critical review of history, concepts, design, applications, and perspectives. *Actuators, 6*(1), 7. https://doi.org/10.3390/act6010007
80. Wang, L., Chen, W. S., Liu, J. K., Deng, J., & Liu, Y. X. (2019). A review of recent studies on non-resonant piezoelectric actuators. *Mechanical Systems and Signal Processing, 133*, 106254. https://doi.org/10.1016/j.ymssp.2019.106254
81. Yang, Z. X., Zhou, X. Q., Huang, H., Dong, J. S., Fan, Z. Q., & Zhao, H. W. (2019). On the suppression of the backward motion of a piezo-driven precision positioning platform designed by the parasitic motion principle. *IEEE Transactions on Industrial Electronics, 67*(5), 3870–3878. https://doi.org/10.1109/TIE.2019.2916295

82. Mohith, S., Upadhya, A. R., Navin, K. P., Kulkarni, S. M., & Rao, M. (2021). Recent trends in piezoelectric actuators for precision motion and their applications: A review. *Smart Materials and Structures, 30*(1), 013002. https://doi.org/10.1088/1361-665X/abc6b9
83. Salim, M., Salim, D., Chandran, D., Aljibori, H. S., & Kherbeet, A. S. (2018). Review of nano piezoelectric devices in biomedicine applications. *Journal of Intelligent Material Systems and Structures, 29*(10), 2105–2121. https://doi.org/10.1177/1045389X17754272
84. Sun, W. X., Xu, Z., Wang, K. F., Li, X., Tang, J. Y., Yang, Z. J., & Huang, H. (2023). An impact inertial piezoelectric actuator designed by means of the asymmetric friction. *IEEE Transactions on Industrial Electronics, 70*(1), 699–708. https://doi.org/10.1109/TIE.2022.3153807
85. Ding, Z. C., Dong, J. S., Zhou, X. Q., Xu, Z., Qiu, W., & Shen, C. L. (2022). Achieving smooth motion of stick–slip piezoelectric actuator by means of alternate stepping. *Mechanical Systems and Signal Processing, 181*, 109494. https://doi.org/10.1016/j.ymssp.2022.109494
86. Yang, Z. X., Zhou, X. Q., & Huang, H. (2022). Design, analysis and experiments of a stick-slip piezoelectric actuator working under the self-deformation mode. *Smart Materials and Structures, 31*(10), 105010. https://doi.org/10.1088/1361-665X/ac8b48
87. Shao, Y., Shao, S. B., Zhai, C. P., Song, S. Y., Han, W. W., Xu, M. L., & Ren, B. (2022). Development of a frequency-controlled inertial type piezoelectric locomotion method with nano-scale motion resolution driven by a symmetrical waveform. *Mechanical Systems and Signal Processing, 177*, 109271. https://doi.org/10.1016/j.ymssp.2022.109271
88. Sun, W. X., Liu, Y. W., Li, X., Xu, Z., Yang, Z. J., & Huang, H. (2022). An inertial impact piezoelectric actuator designed by the asymmetric friction principle and achieved by laser texturing of the driving feet. *Actuators, 11*(8), 211. https://doi.org/10.3390/act11080211
89. Qiao, G. D., Ning, P., Gao, Q., Yu, Y., Lu, X. H., Yang, S. T., & Cheng, T. H. (2022). A flexure hinged mpiezoelectric stick–slip actuator with high velocity and linearity for long-stroke nanopositioning. *Smart Materials and Structures, 31*(7), 075017. https://doi.org/10.1088/1361-665X/ac7428
90. Ji, H. W., Lv, B., Li, Y. H., Yang, F., Qi, A. Q., Wu, X., & Ni, J. (2022). Design and research on tuning fork piezoelectric actuator based on stick-slip effect. *Review of Scientific Instruments, 93*(6), 065007. https://doi.org/10.1063/5.0089052
91. Deng, J., Liu, S. H., Liu, Y. X., Wang, L., Gao, X., & Li, K. (2021). A 2-DOF needle insertion device using inertial piezoelectric actuator. *IEEE Transactions on Industrial Electronics, 69*(4), 3918–3927. https://doi.org/10.1109/TIE.2021.3073313
92. Deng, J., Liu, Y. X., Li, J., Zhang, S. J., & Xie, H. (2022). Influence of multidirectional oscillations on output characteristics of inertial piezoelectric platform. *IEEE/ASME Transactions on Mechatronics, 27*(5), 4122–4131. https://doi.org/10.1109/TMECH.2022.3151102
93. Wang, L., Hou, Y. J., Zhao, K. D., Shen, H., Wang, Z. W., Zhao, C. S., & Lu, X. L. (2019). A novel piezoelectric inertial rotary motor for actuating micro underwater vehicles. *Sensors and Actuators A: Physical, 295*, 428–438. https://doi.org/10.1016/j.sna.2019.06.014
94. Saadabad, N. A., Moradi, H., & Vossoughi, G. (2019). Dynamic modeling, optimized design, and fabrication of a 2DOF piezo-actuated stick-slip mobile microrobot. *Mechanism and Machine Theory, 133*, 514–530. https://doi.org/10.1016/j.mechmachtheory.2018.11.025
95. Zhang, Y. K., Peng, Y. X., Sun, Z. X., & Yu, H. Y. (2018). A novel stick–slip piezoelectric actuator based on a triangular compliant driving mechanism. *IEEE Transactions on Industrial Electronics, 66*(7), 5374–5382. https://doi.org/10.1109/TIE.2018.2868274
96. Wang, X. Y., Zhu, L. M., & Huang, H. (2020). A dynamic model of stick-slip piezoelectric actuators considering the deformation of overall system. *IEEE Transactions on Industrial Electronics, 68*(11), 11266–11275. https://doi.org/10.1109/TIE.2020.3032922
97. Dong, J. S., Zhang, B. W., Li, X. T., Xu, Z., Wang, J. R., Liu, C., & Cao, Y. (2021). A stick-slip piezoelectric actuator with suppressed backward motion achieved using an active locking mechanism (ALM). *Smart Materials and Structures, 30*(9), 095015. https://doi.org/10.1088/1361-665X/ac0cbd
98. Li, J. P., He, L. D., Cai, J. J., Hu, Y. L., Wen, J. M., Ma, J. J., & Wan, N. (2021). A walking type piezoelectric actuator based on the parasitic motion of obliquely assembled PZT stacks. *Smart Materials and Structures, 30*(8), 085030. https://doi.org/10.1088/1361-665X/ac09a0
99. Wang, L., Jin, J. M., Zhang, H. X., Wang, F. Y., & Jiang, Z. (2020). Theoretical analysis and experimental investigation on a novel self-moving linear piezoelectric stepping actuator. *Mechanical Systems and Signal Processing, 135*, 106183. https://doi.org/10.1016/j.ymssp.2019.06.001
100. Bansevicius, R., Mazeika, D., Jurenas, V., Kulvietis, G., & Drukteiniene, A. (2019). Multi-DOF ultrasonic actuators for laser beam positioning. *Shock and Vibration, 2019*, 4919505. https://doi.org/10.1155/2019/4919505